

[Click here to view linked References](#)

Orthogonal Decomposition of Left Ventricular Remodelling in Myocardial Infarction

Xingyu Zhang¹, MHS, Pau Medrano-Gracia¹, PhD, Bharath Ambale-Venkatesh², PhD, David A Bluemke³, MD, Brett R Cowan¹, MBChB, J Paul Finn⁴, MD, Alan H Kadish⁵, MD, Daniel C Lee⁵, MD, Joao AC Lima², MD, Alistair A Young¹, PhD, Avan Suinesiaputra¹, PhD.

¹ Department of Anatomy and Medical Imaging, University of Auckland, Auckland, New Zealand,

² The Donald W. Reynolds Cardiovascular Clinical Research Center, The Johns Hopkins University, Baltimore, USA.

³ National Institute of Biomedical Imaging and Bioengineering, Bethesda, Maryland, USA,

⁴ Department of Radiology, UCLA, Los Angeles, USA.

⁵ Feinberg Cardiovascular Research Institute, Northwestern University Feinberg School of Medicine, Chicago, USA

23 **Abstract**

24 **Background:** Left ventricular size and shape is important for quantifying cardiac
25 remodelling in response to cardiovascular disease. Geometric *remodelling indices* have been
26 shown to have prognostic value in predicting adverse events in the clinical literature, but
27 these do not independently describe shape changes. We developed a novel method for
28 deriving orthogonal shape components directly from any set of clinical indices. Six clinical
29 remodelling indices (end-diastolic volume index, sphericity, relative wall thickness, ejection
30 fraction, apical conicity and longitudinal shortening) were evaluated using cardiac magnetic
31 resonance images of 300 patients with myocardial infarction, and 1,991 asymptomatic
32 subjects, obtained from the Cardiac Atlas Project.

33 **Results:** Partial least squares (PLS) regression of left ventricular shape models resulted in
34 shape components that were optimally associated with each remodelling index. A Gram–
35 Schmidt orthogonalization process, by which components were removed from the shape
36 space in order of variance explained, resulted in a set of orthogonal shape components. A
37 single PLS hidden variable per clinical index resulted in the greatest decorrelation between
38 scores, and complete decorrelation with all previously removed remodelling indices.

39 **Conclusions:** The PLS orthogonal remodelling components had similar power to describe
40 differences between patients and subjects as principal component analysis, but were more
41 correlated to well-understood clinical indices of cardiac remodelling. The data and analyses
42 are available from www.cardiacatlas.org.

43 **Keywords:** cardiac remodelling, magnetic resonance imaging, feature extraction, partial least
44 squares regression.

45 **Background**

1
2
3 46 Left ventricular (LV) remodelling refers to the process by which the heart adapts its size,
4
5 47 shape and function in response to disease processes, or under the influence of mechanical,
6
7 48 neurohormonal and genetic factors [1]. Remodelling can be compensatory, for example
8
9
10 49 increased concentric hypertrophy in hypertension, or adverse, for example increased end-
11
12 50 systolic volume after myocardial infarction. Adverse LV remodelling characteristics after
13
14
15 51 myocardial infarction provide important diagnostic and prognostic information for the
16
17 52 therapeutic management of disease progression [2-5]. Clinical studies have identified
18
19
20 53 quantitative geometric parameters (termed *remodelling indices* in this paper) that describe
21
22 54 recognised clinical patterns of remodelling with prognostic value for predicting adverse
23
24
25 55 events. For example, increased LV volume index has been shown to be an important
26
27 56 predictor of mortality after myocardial infarction [6]. Increased LV sphericity has also been
28
29
30 57 linked with decreased survival [5]. Relative LV wall thickness [1] and apical conicity [7] are
31
32 58 also important indices of adverse remodelling after myocardial infarction. Functional
33
34
35 59 parameters such as ejection fraction (EF), which is the most common index of cardiac
36
37 60 function performance in clinical practice, are also heavily influenced by the degree of LV
38
39 61 remodelling [8, 9]. LV longitudinal shortening is also a sensitive marker of LV remodelling
40
41
42 62 [10].

43
44
45 63 Although these clinical remodelling indices have validated prognostic value, they are often
46
47 64 co-dependent and do not provide an orthogonal decomposition of cardiac shape. Such an
48
49
50 65 orthogonal decomposition would enable computational analysis of the independent
51
52 66 components of remodelling present in various forms of heart disease. In particular,
53
54
55 67 orthogonal shape decompositions enable simplified tensor calculus in the computation of e.g.
56
57 68 arc lengths and areas, because they do not present off-diagonal terms in their metric tensor
58
59
60 69 [11]. An orthogonal basis for shape enables robust calculation of contribution of each

1
2
3
4
5
6
7
8
9
10
11
12
13
14
15
16
17
18
19
20
21
22
23
24
25
26
27
28
29
30
31
32
33
34
35
36
37
38
39
40
41
42
43
44
45
46
47
48
49
50
51
52
53
54
55
56
57
58
59
60
61
62
63
64
65

70 component independently to the overall shape. Also, regressions using orthogonal shape
71 components as independent variables do not suffer from the problem of multicollinearity.
72 Thus, when analysing the combined effects of different remodelling characteristics, it is
73 preferred to have an orthogonal basis in a linear space.

74 Principal component analysis (PCA) [12] is a powerful and widely used shape analysis
75 technique that provides an orthogonal linear shape basis. In previous work, PCA analysis of
76 cardiac remodelling has achieved more powerful descriptions of remodelling, and their
77 relationships with risk factors, than traditional mass and volume analysis [13]. In a large
78 population study, the first and second PCA components corresponded with LV size and
79 sphericity respectively [14]. However, PCA shape components do not generally relate to
80 clinical remodelling indices, making clinical interpretation of the relative contribution of
81 shape components difficult. Remme *et al.* [15] developed a method to decompose shape
82 changes into modes with clear clinical interpretation. However, these modes were not
83 orthogonal.

84 In this paper, we used partial least squares (PLS) regression to sequentially construct an
85 orthogonal shape decomposition that is optimally related to clinical remodelling indices. At
86 each step, the contribution of the previous component was removed mathematically from the
87 shape description, similar to Gram–Schmidt orthogonalization. Clinical remodelling indices
88 of end-diastolic volume index (EDVI), sphericity, ejection fraction, relative wall thickness,
89 conicity and longitudinal shortening, known from the literature to have important prognostic
90 information in the management of myocardial infarction, were used to create corresponding
91 orthogonal components from the shape parameters. By using a single PLS hidden variable per
92 clinical index, the resulting component scores were maximally de-correlated, and completely
93 de-correlated with those clinical indices previously removed.

94 **Data Description**

95 *Patient Data*

96 LV shape models of 300 patients with myocardial infarction and 1,991 asymptomatic study
97 subjects were obtained through the Cardiac Atlas Project [16]. The patient data have been
98 described previously [13] [17] and are available from the Cardiac Atlas Project
99 (<http://www.cardiacatlas.org>). Briefly, myocardial infarction patients (n=300, age 31–86,
100 mean age 63, 20% women) had clinical history of myocardial infarction with EF>35% and
101 infarct mass >10% of LV myocardial mass. Asymptomatic subjects (n=1991, age 45–84,
102 mean age 61, 52% women) did not have physician-diagnosed heart attack, angina, stroke,
103 heart failure or atrial fibrillation, and had not undergone procedures related to cardiovascular
104 disease, at the time of recruitment [13] [17].

105 Finite element shape models were customized to cardiac MRI exams in each case using a
106 standardized procedure [13]. The shape models were evenly sampled at sufficient resolution
107 to capture all visible features, which resulted in 1,682 Cartesian (x_i, y_i, z_i) points in
108 homologous anatomical locations for each LV model.

109 *Clinical Remodelling Indices*

110 Clinical remodelling indices included EDVI, EF, relative wall thickness, sphericity, apical
111 conicity and longitudinal shortening. LV mass and volumes were calculated by numerical
112 integration of the LV shape models. EDVI was calculated as EDV divided by body surface
113 area. Ejection fraction was calculated as $(EDV-ESV)/EDV$. Relative wall thickness was
114 defined as twice the posterior wall thickness divided by the end-diastolic diameter [18] at
115 mid-ventricle. Sphericity was calculated as the EDV divided by the volume of a sphere with a
116 diameter corresponding to the major axis at end-diastole in LV long axis view [19]. Apical
117 conicity was calculated as the ratio of the apical diameter (defined as the diameter of the

118 endocardium one third above the apex) over the basal diameter [7] at end-diastole.

119 Longitudinal shortening was calculated as the difference of the distance of the central basal
120 point to the apical point at end-diastole and end-systole over the distance at end-diastole.

121 *Partial Least Squares Regression*

122 Partial least squares (PLS) regression [20, 21] is a statistical method that is related to
123 principal components regression; however, instead of using independent variables derived
124 from their ability to explain variance in the predictive variables only, PLS finds independent
125 variables by projecting both the predicted variables and the predictor variables to a new space,
126 typically with reduced dimension, chosen to maximize the correlation between predicted and
127 predictor variables. PLS is typically used to find the fundamental relations between the
128 predicted and predictor variables, i.e. a latent variable approach to modelling the covariance
129 structures in these two spaces.

130 Mathematically, let X represent the data matrix where each row contains the coordinates of
131 3D points describing the shape of one case at ED, concatenated with the points at ES. In our
132 application all asymptomatic and myocardial infarction cases were included in this matrix.
133 Given a vector of clinical remodeling indices (e.g. EDVI) denoted as Y , PLS finds a linear
134 decomposition of both X and Y such that

$$135 \begin{aligned} X &= TP^T + E \\ Y &= UQ^T + F \end{aligned}$$

136 where T and U are, respectively, the projections of X and Y (also termed *scores*); P and Q are
137 the loading matrices of reduced dimensionality N_{latent} (i.e. the number of latent variables used
138 in the PLS decomposition) and E and F are the error terms assumed to be independent and
139 identically distributed random normal variables. This decomposition is optimised to
140 maximise the covariance between T and U [20].

141 The regression coefficients are also calculated so that $Y = [1 \ X]B + Y_{residuals}$, where B is
142 a matrix of coefficients including the intercept. In this paper we used the SIMPLS algorithm
143 as provided by the Statistics and Machine Learning Toolbox (MATLAB R2013a, The
144 MathWorks, Inc., Natick, Massachusetts, United States). In this implementation T is
145 orthonormal, but P , Q and U are not. However, each column of U is orthogonalised with
146 respect to preceding columns of T , so that $T^T U$ is lower triangular.

147 *Orthogonalization of PLS Components*

148 The orthogonal remodelling components were created using PLS sequentially as shown in
149 Figure 1. EDVI was selected as the first component, because it accounts for the greatest
150 variance in the LV shape [13]. The contribution of this component was then removed from
151 the shape description, by using a mathematical formulation similar to the Gram–Schmidt
152 orthogonalization algorithm [22], prior to the calculation of the following components. This
153 step ensures orthogonality in the new shape basis. The other remodelling components were
154 calculated by PLS regression to the remaining clinical indices, using the deflated shape space.
155 The component explaining the greatest variance in shape was then chosen as the next
156 component to be removed from the shape space. This procedure was performed iteratively
157 until all components were explained. The final order of the components was: (1) EDVI, (2)
158 sphericity, (3) ejection fraction, (4) relative wall thickness, (5) conicity and (6) longitudinal
159 shortening.

160 Following Figure 1, using super-indices to enumerate steps and sub-indices for columns, let
161 $X = X^0$, the original shape space, and $Y = Y^1$, the first clinical index, i.e. EDVI. After the
162 PLS regression, we define our “PLS component” as the normalized PLS regression
163 coefficients B^1 omitting the intercept term. This is a vector in shape space that is maximally

164 correlated with EDVI. The projections associated with that component are X^0B^1 , and these
165 were used as the component scores in the remodelling analysis below.

166 The shape space is then deflated by the EDVI-derived PLS component, giving rise to a new
167 data matrix $X^1: X^1=X^0 - X^0B^1(B^1)^T$. The next clinical index is then chosen as the one that
168 explains the most variation of the population in the new shape space, and the PLS regression
169 and deflation are repeated for the remaining indices Y^k where at each step the previous PLS
170 component contribution is removed:

$$X^k=X^{k-1} - X^{k-1}B^k(B^k)^T$$

172 Note that subsequent B^{k+1} will be orthogonal to B^k by construction since X^{k+1} is orthogonal
173 to B^k . Therefore the set of basis vectors B^k generate an orthogonal linear sub-space of X^0 .

174 *Number of latent variables*

175 Selection of the number of latent variables N_{latent} is critical for obtaining PLS regression
176 models with good predictive ability [23]. However, there is currently no standard method to
177 choose the number of latent variables for PLS. We compared PLS regression results with
178 $N_{latent} =1$ and $N_{latent} =10$. Results for $N_{latent} >10$ were similar to $N_{latent} =10$ because 10 latent
179 variables accounted for most of the covariance between Y and X. Experiments for
180 $1 < N_{latent} < 10$ gave intermediate results.

181 *Characterization of myocardial infarction*

182 To assess the clinical applicability of the orthogonal remodelling components, we analysed
183 how these components were associated with myocardial infarction. Logistic regression
184 models [24] were used to evaluate the discriminatory power of the orthogonal remodelling
185 components to characterize LV remodelling due to myocardial infarction. Confounding

186 factors (age, gender, BMI, SBP, smoking status and diabetes history) were included in each
187 regression model as baseline variables (covariates). Four logistic regression models were
188 examined. Model 1 consisted of the baseline variables and the first 6 PCA scores. This was
189 used as a reference for comparison. Model 2 consisted of the baseline variables and the
190 clinical remodelling indices. Model 3 included the baseline variables and the orthogonal
191 component scores for $N_{latent} = 1$. Model 4 included the baseline variables and the orthogonal
192 component scores for $N_{latent} = 10$.

193 Four commonly-used measures were used to quantify the goodness-of-fit of the regression
194 models: Deviance, Akaike information criterion (AIC), Bayesian information criterion (BIC)
195 and the area under the receiver operating characteristic curve (AUC) [13]. Smaller Deviance,
196 AIC and BIC, and larger AUC, are indicative of better goodness-of-fit.

197 **Analyses**

198 Participant characteristics are summarised in Table 1. Demographic characteristics were
199 significantly different between the asymptomatic subjects and the myocardial infarction cases,
200 including gender ratio, age, height, weight, blood pressure, diabetes history and smoking
201 status. Clinical LV remodelling indices were also significantly different. The myocardial
202 infarction patients had larger LV EDVI and ESV, increased sphericity, thicker walls, less
203 conicity, smaller EF and reduced longitudinal shortening than the asymptomatic subjects.

204 The orthogonal PLS components corresponding to EDVI, sphericity, ejection fraction,
205 relative wall thickness, conicity and longitudinal shortening, computed across all patient and
206 asymptomatic cases, are shown in Figure 2 ($N_{latent} = 1$) and Figure 3 ($N_{latent} = 10$). Linear
207 correlation coefficients were calculated between the clinical indices and the component
208 scores in the combined population. Linear correlation coefficients between all PLS
209 component scores and clinical indices are reported in Table 2 for $N_{latent} = 1$ and in Table 3 for

210 $N_{latent}=10$. The linear correlation coefficients among the clinical indices are shown in Table 4,
211 among the PLS component scores are shown in Table 5 for $N_{latent}=1$ and in Table 6 for N_{latent}
212 $=10$. Correlation coefficients between clinical indices and scores of the first six PCA
213 components of the original dataset are shown in Table 7 for comparison with PLS
214 components in Tables 2 and 3.

215 The minimum correlation between remodelling scores was achieved with $N_{latent}=1$ (Table 5),
216 because the PLS regression with only one latent variable finds the single shape vector that is
217 maximally correlated with the clinical index. A single latent variable also resulted in
218 complete decorrelation between the remodelling scores and the remodelling indices of all the
219 components previously removed in the Gram-Schmidt procedure (Table 2).

220 Using more latent variables resulted in a subspace that yielded better correlation between
221 each score and its corresponding index (diagonal elements are higher in Table 3 than in Table
222 2). However the deflated shape space retains correlation with the index.

223 Figure 4 shows the shape variance explained by each one of the PLS components for $N_{latent}=1$,
224 $N_{latent}=10$ and by PCA. The total variance explained was the highest for PCA components
225 (75.7% for 6 components). For PLS with $N_{latent}=1$, variance explained was 66.49% for 6
226 components, whereas for $N_{latent}=10$ it was 15.0%. This reflects the fact that PLS is designed
227 to explain covariance between indices and shapes, rather than variance in the shapes
228 themselves.

229 The results of logistic regression models to characterize remodelling associated with
230 myocardial infarction using the orthogonal remodelling components are shown in Table 8.

231 The scores from all orthogonal remodelling components showed significant odds ratios. The
232 odds ratio of EDVI, sphericity, wall thickness, conicity, ejection fraction and longitudinal

1
2
3
4
5
6
7
8
9
10
11
12
13
14
15
16
17
18
19
20
21
22
23
24
25
26
27
28
29
30
31
32
33
34
35
36
37
38
39
40
41
42
43
44
45
46
47
48
49
50
51
52
53
54
55
56
57
58
59
60
61
62
63
64
65

233 shortening component scores indicate that myocardial infarction patients tend to have larger
234 and more spherical LV shapes with thinner walls, and a less conical shape.

235 Table 9 shows the comparisons of the regression models with the baseline models. All three
236 regression models showed significant improvement compared with the baseline model. The
237 logistic regression based on orthogonal remodelling components showed smaller Deviance,
238 AIC and BIC and higher AUC than the PCA logistic regression. The AUC (Figure 5) for the
239 PLS components with a single latent variable was 97.38%, slightly greater than that for the
240 PLS components with 10 latent variables (95.99%), or the logistic classification using scores
241 from the first 6 PCA components (97.28%), or the logistic classification using the
242 corresponding clinical indices (95.96%). The PLS components with a single latent variable
243 (Model 3) obtained the best classification power and goodness-of-fit measures.

244 The standardized coefficients of the logistic regression model were used to create a linear
245 combination of the PLS ($N_{latent} = 1$) components generating a combined remodelling score,
246 called the LR score (Figure 6), separating the two groups. The median LR scores (Model 3)
247 for all cases were calculated and the median shapes were calculated by projecting the
248 coefficients of the PLS components estimated in the logistic regression model back on the
249 population shape space. These are plotted in Figure 6. This graphically shows the shape
250 changes which best distinguish the two groups with baseline variables adjusted, showing that
251 LV remodelling due to myocardial infarction is associated with larger volume, more spherical
252 shape, and thinner wall thickness. Since the logistic regression coefficients refer to
253 contributions from remodelling components, the amount of each remodelling component
254 contributing to the LR score could be quantified. This gives an intuitive explanation of the
255 LR score in terms of remodelling components associated with clinical remodelling indices.

Discussion

Patients with myocardial infarction exhibit significant shape changes with respect to the normal population, due to cardiac remodelling. An atlas-based analysis of cardiac remodelling has previously shown better characterization of remodelling due to myocardial infarction than traditional mass and volume analysis in large data sets [13]. The framework consisted of three steps: (1) fitting a finite element model to the LV MR images, (2) feature extraction of the aligned shape parameters, and (3) quantification of the association between the features and disease using logistic regression. Although PCA provides orthogonal shape features, which describe the maximum amount of variation for the fewest number of components, these components typically do not correspond with clinical indices of cardiac remodelling. To avoid this problem, and maintain the advantages of orthogonality, we developed a method to generate orthogonal shape components from any set of clinical indices using PLS.

In this paper, we generated a linear orthogonal shape basis from the full finite element shape parameters. Clinical indices, such as EDVI, sphericity, ejection fraction, relative wall thickness, conicity and longitudinal shortening, were derived from the finite element shape model. Similar to PCA, the shape components derived from PLS regression are orthogonal (zero dot product between different component shape vectors). In PCA, the resulting component scores are also decorrelated across the population cohort, but this is not the case with PLS. Table 6 shows that PLS component scores with $N_{latent} = 10$ were significantly correlated, similar to the original clinical indices in Table 4. This is expected since $N_{latent} = 10$ results in strong correlations between scores and indices (Table 3). PLS components both using $N_{latent} = 10$ and $N_{latent} = 1$ obtain effective shape representation for each clinical index, as evidenced by the correlation coefficients with the clinical indices (diagonal terms in Tables 2 and 3). However correlations between the scores of different indices for PLS with $N_{latent} = 1$

1
2
3
4
5
6
7
8
9
10
11
12
13
14
15
16
17
18
19
20
21
22
23
24
25
26
27
28
29
30
31
32
33
34
35
36
37
38
39
40
41
42
43
44
45
46
47
48
49
50
51
52
53
54
55
56
57
58
59
60
61
62
63
64
65

281 become smaller than the original indices and scores of PLS with $N_{latent} = 10$. For example, the
282 correlation between EDVI and EF was originally -0.60 (Table 4), then became -0.68 from
283 PLS with $N_{latent} = 10$ (Table 6); however it was -0.15 from PLS with $N_{latent} = 1$ (Table 5).

284 Not only did a single latent variable result in the greatest decorrelation between component
285 scores (Table 5), but it also resulted in total decorrelation between component scores and
286 previously removed indices (upper triangle of Table 2).

287 These orthogonal components derived from traditional remodelling indices may be used to
288 partition shape into contributions from each component, independent of the others.
289 Correlation analysis shows that these clinically derived components have high
290 correspondence with traditional remodelling indices (diagonals in Tables 2 and 3), either
291 virtually following the clinical indices' original correlation (Table 4) in $N_{latent} = 10$ (Table 3),
292 or by sacrificing some of the diagonal correlations in exchange for decoupling with previous
293 indices in $N_{latent} = 1$ (Table 2). Shapes features at $N_{latent} = 10$ are more correlated with the
294 original clinical indices than $N_{latent} = 1$ but at the expense of their ability to explain variance in
295 the original shape space (Figure 7). It can therefore be argued that $N_{latent} = 10$ generates more
296 'specific' shapes with lesser representative power.

297 The results also show that clinically derived components quantitatively characterise
298 remodelling features associated with myocardial infarction with similar power as PCA
299 components. Three logistic regression models based on the clinical indices, PCA components
300 and orthogonal remodelling components derived from clinical indices were all similar in
301 terms of goodness of fit.

302 Coefficients of the PLS components estimated in the logistic regression model were projected
303 back on the population shape space. By projecting these components back onto the
304 population space (Figure 5), we can visualise the shape changes of the six features (the

1
2
3
4
5
6
7
8
9
10
11
12
13
14
15
16
17
18
19
20
21
22
23
24
25
26
27
28
29
30
31
32
33
34
35
36
37
38
39
40
41
42
43
44
45
46
47
48
49
50
51
52
53
54
55
56
57
58
59
60
61
62
63
64
65

305 change of EDVI, sphericity, EF, RWT, conicity and longitudinal shortening) due to
306 remodelling. This combined component can be used for tracking individual patients over time
307 in future studies, by quantifying the degree to which their LV shapes compare with the
308 remodelling spectrum.

309 Supervised feature extraction techniques such as information maximising component analysis
310 and linear discriminate analysis have also been used to extract a remodelling component
311 which can best characterize myocardial infarction using surface sampling [25]. In the current
312 study, the shape features of each clinical index were obtained first and then combined using
313 logistic regression with baseline information removed. The shape changes due to myocardial
314 infarction obtained by this LR model can be more easily explained as a combination of well-
315 understood shape features, through the LR coefficients.

316 This method can be applied to any index with particular clinical utility, with visualization of
317 their corresponding shape features and quantification of components, thereby further
318 exploiting shape information in a clinically meaningful fashion.

319 **Potential implications**

320 This work enables precise multi-dimensional characterization of the ways in which the heart
321 adapts with the progression of disease after myocardial infarction. The computed shape
322 components are clinically meaningful since they are optimally related to indices with proven
323 prognostic value. The resulting shape component scores can be used to track the progression
324 of remodelling over time, against reference populations. This enables automatic computation
325 of z-scores giving precise information on how the patient's heart compares against the
326 reference population.

327 **Availability of supporting data and materials**

1
2
3
4
5
6
7
8
9
10
11
12
13
14
15
16
17
18
19
20
21
22
23
24
25
26
27
28
29
30
31
32
33
34
35
36
37
38
39
40
41
42
43
44
45
46
47
48
49
50
51
52
53
54
55
56
57
58
59
60
61
62
63
64
65

328 LV shape models, clinical indices and orthogonal shape modes, together with code for their
329 calculation and visualization, are available for public download at
330 <http://www.cardiacatlas.org/tools/lv-shape-orthogonal-clinical-modes/>. Information on the
331 original imaging studies can be found at <http://www.cardiacatlas.org/studies/>. DICOM image
332 data and associated clinical variables are obtainable on request at
333 <http://www.cardiacatlas.org/data-access/request-cap-access/>. Because of the variety of
334 sources of imaging data, each with different IRB and steering committee requirements, the
335 DICOM images and associated clinical information are not publically available; however,
336 these data are made available to researchers on approval of a research application submitted
337 under the Cardiac Atlas Project data sharing policy (www.cardiacatlas.org).

338

339 **Declarations**

340 **Abbreviations and Acronyms**

341 Left ventricular =LV, Ejection Fraction = EF, Principal Component Analysis = PCA, Partial
342 Least Squares = PLS, End-diastolic Volume Index (EDVI), End-systolic Volume = ESV,
343 Myocardial infarction =MI, Ejection fraction =EF, Longitudinal shortening =LS, End-
344 systolic volume = ESV, end-diastolic volume = EDV, LV mass =LVM, left ventricle mass
345 index= LVMI, Relative wall thickness = RWT, mass to volume ratio =MVR, Systolic Blood
346 Pressure=SBP, Diastolic blood pressure=DBP

347 **Ethics approval and consent to participate**

348 This study was approved by the local institutional review boards (Johns Hopkins University
349 School of Medicine NA_00031350; Northwestern University CR1_STU00000078; New

1
2
3
4
5
6
7
8
9
10
11
12
13
14
15
16
17
18
19
20
21
22
23
24
25
26
27
28
29
30
31
32
33
34
35
36
37
38
39
40
41
42
43
44
45
46
47
48
49
50
51
52
53
54
55
56
57
58
59
60
61
62
63
64
65

350 Zealand Multi-region Ethics Committee MEC/08/04/052) and all participants gave written
351 informed consent.

352 **Consent for Publication**

353 Not applicable

354 **Competing interests**

355 None

356 **Funding**

357 This project was supported by award numbers R01HL087773 and R01HL121754 from the
358 National Heart, Lung, and Blood Institute. MESA was supported by contracts N01-HC-95159
359 through N01-HC-95169 from the NHLBI and by grants UL1-RR-024156 and UL1-RR-
360 025005 from NCRR. DETERMINE was supported by St. Jude Medical, Inc; and the National
361 Heart, Lung and Blood Institute (R01HL91069). David A. Bluemke is supported by the NIH
362 intramural research program. Xingyu Zhang was supported by the China Scholarship Council.

363 **Authors' contributions**

364 All authors were involved in the design of the study, interpretation of the data, drafting and
365 revision of the manuscript, and final approval of the submitted manuscript. XZ, PM-G, and
366 AS performed the statistical analyses.

367 **Authors' Information**

368 XZ is a PhD student and biostatistician. PM-G is a biostatistician and expert in bioinformatics.
369 BA-V is a bioengineer and expert in medical image analysis. DB is a radiologist and Director
370 of Radiology and Imaging Sciences at the National Institute of Biomedical Imaging and
371 Bioengineering and a co-PI of the MESA study. BR is a clinical engineer and an expert in

1
2
3
4
5
6
7
8
9
10
11
12
13
14
15
16
17
18
19
20
21
22
23
24
25
26
27
28
29
30
31
32
33
34
35
36
37
38
39
40
41
42
43
44
45
46
47
48
49
50
51
52
53
54
55
56
57
58
59
60
61
62
63
64
65

372 cardiac MRI. JPF is a radiologist and Director of Magnetic Resonance Research at UCLA
373 and a co-PI of the DETERMINE study. AK is a cardiologist and PI of the DETERMINE
374 study; DL is a cardiologist and Director of the DETERMINE MRI Core Lab. JL is a
375 cardiologist and Director of the MESA MRI Core Lab. AY is a bioengineer and PI of the
376 Cardiac Atlas Project and head of Department of Anatomy and Medical Imaging at the
377 University of Auckland. AS is an expert in atlas-based medical image analysis.

References

1. Sutton MGSJ, Sharpe N: **Left Ventricular Remodeling After Myocardial Infarction: Pathophysiology and Therapy.** *Circulation* 2000, **101**:2981-2988.
2. Gjesdal O, Bluemke DA, Lima JA: **Cardiac remodeling at the population level[mdash]risk factors, screening, and outcomes.** *Nat Rev Cardiol* 2011, **8**:673-685.
3. Lieb W, Gona P, Larson MG, Aragam J, Zile MR, Cheng S, Benjamin EJ, Vasan RS: **The Natural History of Left Ventricular Geometry in the CommunityClinical Correlates and Prognostic Significance of Change in LV Geometric Pattern.** *JACC: Cardiovascular Imaging* 2014, **7**:870-878.
4. Zile MR, Gaasch WH, Patel K, Aban IB, Ahmed A: **Adverse left ventricular remodeling in community-dwelling older adults predicts incident heart failure and mortality.** *JACC: Heart Failure* 2014.
5. Wong SP, French JK, Lydon A-M, Manda SOM, Gao W, Ashton NG, White HD: **Relation of left ventricular sphericity to 10-year survival after acute myocardial infarction.** *The American journal of cardiology* 2004, **94**:1270-1275.
6. White HD, Norris RM, Brown MA, Brandt PW, Whitlock RM, Wild CJ: **Left ventricular end-systolic volume as the major determinant of survival after recovery from myocardial infarction.** *Circulation* 1987, **76**:44-51.
7. Di Donato M, Dabic P, Castelvechio S, Santambrogio C, Brankovic J, Collarini L, Joussef T, Frigiola A, Buckberg G, Menicanti L, the RG: **Left ventricular geometry in normal and post-anterior myocardial infarction patients: sphericity index and ‘new’ conicity index comparisons.** *European Journal of Cardio-Thoracic Surgery* 2006, **29**:S225-S230.
8. Konstam MA, Kramer DG, Patel AR, Maron MS, Udelson JE: **Left Ventricular Remodeling in Heart FailureCurrent Concepts in Clinical Significance and Assessment.** *JACC: Cardiovascular Imaging* 2011, **4**:98-108.
9. Anand I, McMurray J, Cohn JN, Konstam MA, Notter T, Quitzau K, Ruschitzka F, Lüscher TF: **Long-term effects of darusentan on left-ventricular remodelling and clinical**

406 **outcomes in the Endothelin A Receptor Antagonist Trial in Heart Failure (EARTH):**
 1
 2 407 **randomised, double-blind, placebo-controlled trial.** *The Lancet* 2004, **364**:347-354.
 3
 4 408 10. Kramer CM, Lima JA, Reichek N, Ferrari VA, Llaneras MR, Palmon LC, Yeh IT, Tallant B,
 5
 6 409 Axel L: **Regional differences in function within noninfarcted myocardium during left**
 7
 8 410 **ventricular remodeling.** *Circulation* 1993, **88**:1279-1288.
 9
 10
 11 411 11. Syngne JL, Schild A: *Tensor calculus.* Courier Corporation; 1969.
 12
 13 412 12. Jolliffe I: *Principal component analysis.* Wiley Online Library; 2005.
 14
 15 413 13. Zhang X, Cowan BR, Bluemke DA, Finn JP, Fonseca CG, Kadish AH, Lee DC, Lima JAC,
 16
 17 414 Suinesiaputra A, Young AA, Medrano-Gracia P: **Atlas-Based Quantification of Cardiac**
 18
 19 415 **Remodeling Due to Myocardial Infarction.** *PLoS ONE* 2014, **9**:e110243.
 20
 21
 22 416 14. Medrano-Gracia P, Cowan BR, Ambale-Venkatesh B, Bluemke DA, Eng J, Finn JP, Fonseca
 23
 24 417 CG, Lima JAC, Suinesiaputra A, Young AA: **Left ventricular shape variation in**
 25
 26 418 **asymptomatic populations: the multi-ethnic study of atherosclerosis.** *Journal of*
 27
 28 419 *Cardiovascular Magnetic Resonance* 2014, **16**:56.
 29
 30
 31 420 15. Remme EW, Young AA, Augenstein KF, Cowan B, Hunter PJ: **Extraction and**
 32
 33 421 **quantification of left ventricular deformation modes.** *IEEE Trans Biomed Eng* 2004,
 34
 35 422 **51**:1923-1931.
 36
 37
 38 423 16. Fonseca CG, Backhaus M, Bluemke DA, Britten RD, Do Chung J, Cowan BR, Dinov ID,
 39
 40 424 Finn JP, Hunter PJ, Kadish AH: **The Cardiac Atlas Project—an imaging database for**
 41
 42 425 **computational modeling and statistical atlases of the heart.** *Bioinformatics* 2011, **27**:2288-
 43
 44 426 2295.
 45
 46
 47 427 17. Medrano-Gracia P, Cowan BR, Bluemke DA, Finn JP, Kadish AH, Lee DC, Lima JAC,
 48
 49 428 Suinesiaputra A, Young AA: **Atlas-based analysis of cardiac shape and function:**
 50
 51 429 **correction of regional shape bias due to imaging protocol for population studies.** *Journal*
 52
 53 430 *of Cardiovascular Magnetic Resonance* 2013, **15**:80.
 54
 55
 56 431 18. Li L, Shigematsu Y, Hamada M, Hiwada K: **Relative Wall Thickness Is an Independent**
 57
 58 432 **Predictor of Left Ventricular Systolic and Diastolic Dysfunctions in Essential**
 59
 60 433 **Hypertension.** *Hypertension Research* 2001, **24**:493-499.
 61
 62
 63
 64
 65

1
2
3
4
5
6
7
8
9
10
11
12
13
14
15
16
17
18
19
20
21
22
23
24
25
26
27
28
29
30
31
32
33
34
35
36
37
38
39
40
41
42
43
44
45
46
47
48
49
50
51
52
53
54
55
56
57
58
59
60
61
62
63
64
65

434 19. Izumo M, Lancellotti P, Suzuki K, Kou S, Shimozato T, Hayashi A, Akashi YJ, Osada N,
435 Omiya K, Nobuoka S, et al: *Three-dimensional echocardiographic assessments of exercise-*
436 *induced changes in left ventricular shape and dyssynchrony in patients with dynamic*
437 *functional mitral regurgitation.* 2009.

438 20. Geladi P, Kowalski BR: **Partial least-squares regression: a tutorial.** *Analytica chimica acta*
439 1986, **185**:1-17.

440 21. de Jong S, Phatak A: **Partial least squares regression.** *Recent advances in total least squares*
441 *techniques and errors-in-variables modeling* 1997:311-338.

442 22. Hoffmann W: **Iterative algorithms for Gram-Schmidt orthogonalization.** *Computing* 1989,
443 **41**:335-348.

444 23. Gómez-Carracedo MP, Andrade JM, Rutledge DN, Faber NM: **Selecting the optimum**
445 **number of partial least squares components for the calibration of attenuated total**
446 **reflectance-mid-infrared spectra of undesigned kerosene samples.** *Analytica Chimica*
447 *Acta* 2007, **585**:253-265.

448 24. Zhang X, Ambale-Venkatesh B, Bluemke D, Cowan B, Finn JP, Hundley W, Kadish A, Lee
449 D, Lima JC, Suinesiaputra A, et al: **Orthogonal Shape Modes Describing Clinical Indices**
450 **of Remodeling.** In *Functional Imaging and Modeling of the Heart. Volume 9126.* Edited by
451 van Assen H, Bovendeerd P, Delhaas T: Springer International Publishing; 2015: 273-281:
452 *Lecture Notes in Computer Science*].

453 25. Zhang X, Ambale-Venkatesh B, Bluemke D, Cowan B, Finn J, Kadish A, Lee D, Lima J,
454 Hundley W, Suinesiaputra A, et al: **Information maximizing component analysis of left**
455 **ventricular remodeling due to myocardial infarction.** *Journal of Translational Medicine*
456 2015, **13**:343.

459 **Tables**

460
461 **Table 1** Baseline variables and clinical remodelling indices for asymptomatic subjects and
462 patients with myocardial infarction (mean \pm SD)

Variable	Unit	Asymptomatic	MI cases	p-value
Sex	F/M	1034/975	60/238	<0.01
Age	years	61.47 \pm 10.15	62.76 \pm 10.76	0.043
Height	cm	165.98 \pm 9.99	173.82 \pm 9.77	<0.001
Weight	kg	76.75 \pm 16.50	90.06 \pm 14.14	<0.001
BMI		27.77 \pm 5.09	29.73 \pm 5.57	<0.001
SBP	mmHg	126.28 \pm 21.98	126.36 \pm 17.50	>0.05
DBP	mmHg	71.49 \pm 10.33	73.26 \pm 9.82	0.006
Diabetes history	%	13.11	35.67	<0.001
Smoking status	%	12.51	11.33	>0.05
EDVI	ml/m ²	67.83 \pm 13.29	96.53 \pm 25.03	<0.001
Sphericity		0.38 \pm 0.08	0.41 \pm 0.09	<0.001
RWT	%	39.71 \pm 9.49	35.21 \pm 8.38	<0.001
Conicity		0.74 \pm 0.08	0.70 \pm 0.08	<0.001
EF		0.63 \pm 0.07	0.41 \pm 0.11	<0.001
LS		0.13 \pm 0.04	0.08 \pm 0.03	<0.001

463
464 MI=Myocardial infarction; BMI=Body mass index; SBP=Systolic blood pressure; DBP=diastolic
465 blood pressure; EDV= end diastolic volume; RWT=relative wall thickness; EF= ejection fraction;
466 LS=longitudinal shortening.

469 **Table 2** Correlation coefficients between the clinical indices and the PLS component scores

470 $(N_{latent} = 1)$

	EDVI score	Sphericity score	EF score	RWT score	Conicity score	LS score
EDVI	0.82	0	0	0	0	0
Sphericity	0.03	0.83	0	0	0	0
EF	-0.75	0.03	0.61	0	0	0
RWT	-0.20	-0.16	-0.04	0.53	0	0
Conicity	-0.14	-0.28	0.30	0.21	0.72	0
LS	-0.45	0.03	0.61	-0.17	0.20	0.53

471

472 **Table 3** Correlation coefficients between the clinical indices and the PLS component scores

473 $(N_{latent} = 10)$

	EDVI score	Sphericity score	WT score	EF score	Conicity score	LS score
EDVI	0.94	0.27	-0.64	-0.34	-0.13	-0.31
Sphericity	0.30	0.97	-0.16	-0.15	-0.25	-0.13
WT	-0.65	-0.12	0.99	0.26	0.25	0.53
EF	-0.41	-0.28	0.22	0.90	0.25	-0.02
Conicity	-0.13	-0.22	0.25	0.38	0.97	0.24
LS	-0.32	-0.13	0.56	0.02	0.25	0.98

474

475

476

Table 4 Correlation coefficients among the clinical indices.

	EDVI	Sphericity	EF	RWT	Conicity	LS
EDVI	1	0.28	-0.60	-0.37	-0.11	-0.29
Sphericity	0.28	1	-0.11	-0.28	-0.22	-0.13
EF	-0.60	-0.11	1	0.18	0.26	0.57
RWT	-0.37	-0.28	0.18	1	0.32	0.00
Conicity	-0.11	-0.22	0.26	0.32	1	0.26
LS	-0.29	-0.13	0.57	0.00	0.26	1

477

478

Table 5 Correlation coefficients among the PLS clinical modes' scores ($N_{latent}=1$)

	EDVI score	Sphericity score	EF score	RWT score	Conicity score	LS score
EDVI score	1	-0.29	-0.15	0.22	-0.15	-0.08
Sphericity score	-0.29	1	0.001	-0.04	0.01	0.22
EF score	-0.15	0.001	1	0.09	0.09	0.09
RWT score	0.22	-0.04	0.09	1	-0.08	0.002
Conicity score	-0.15	0.01	0.09	-0.08	1	0.16
LS score	-0.08	0.22	0.47	0.002	0.16	1

479

480

Table 6 Correlation coefficients among the PLS clinical mode scores ($N_{latent}=10$)

	EDVI score	Sphericity score	EF score	WT score	Conicity score	LS score
EDVI score	1	0.29	-0.68	-0.37	-0.15	-0.34
Sphericity score	0.29	1	-0.17	-0.15	-0.25	-0.14
EF score	-0.68	-0.17	1	0.27	0.25	0.53
WT score	-0.37	-0.15	0.27	1	0.31	-0.01
Conicity score	-0.15	-0.25	0.25	0.31	1	0.24
LS score	-0.34	-0.14	0.53	-0.01	0.24	1

Table 7 Correlation coefficients between the clinical indices and the first 6 modes of variation of X^0 using PCA

	PC 1	PC 2	PC 3	PC 4	PC 5	PC 6
EDVI	0.80	-0.01	-0.74	-0.18	-0.13	-0.45
Sphericity	-0.26	-0.80	0.19	0.19	0.30	0.06
EF	-0.01	0.09	-0.11	0.03	-0.09	-0.20
RWT	0.10	0.24	-0.21	-0.25	-0.25	-0.18
Conicity	0.10	0.13	-0.15	-0.11	-0.15	-0.14
LS	0.21	0.02	0.03	-0.15	0.50	0.37

Table 8 Four logistic regressions for myocardial infarction

Variable	Coefficient	Standard error	p value	Standardized Coefficient	Odds Ratio(OR)	OR 95% Confidence Interval
Model 1: PCA modes + Baseline model						
PC 1*	2.647	0.177	<.0001	1.459	14.108	9.969 19.967
PC 2*	-0.605	0.102	<.0001	-0.334	0.546	0.447 0.666
PC 3	0.077	0.112	0.492	0.042	1.080	0.867 1.345
PC 4*	2.024	0.153	<.0001	1.116	7.571	5.610 10.217
PC 5*	0.394	0.106	0.0002	0.217	1.483	1.204 1.826
PC 6	-0.115	0.119	0.331	-0.064	0.891	0.706 1.124
Model 2: Clinical indices + Baseline model						
EDVI*	0.042	0.008	<.0001	0.420	1.043	1.028 1.059
Sphericity	0.003	0.014	0.803	0.015	1.003	0.977 1.031
EF	0.002	0.014	0.885	0.011	1.002	0.975 1.030
RWT *	-0.161	0.015	<.0001	-0.948	0.852	0.827 0.877
Conicity*	-0.037	0.016	0.020	-0.159	0.964	0.935 0.994
LS*	-0.148	0.037	<.0001	-0.327	0.862	0.802 0.927
Model 3: PLS modes ($N_{latent}=1$) + Baseline model						
EDVI score*	2.838	0.189	<.0001	1.565	17.078	11.782 24.756
Sphericity score*	0.895	0.125	<.0001	0.494	2.448	1.917 3.126
EF score*	-1.315	0.148	<.0001	-0.725	0.269	0.201 0.359
RWT score	-1.542	0.149	<.0001	-0.850	0.214	0.160 0.286
Conicity score	0.343	0.124	0.006	0.189	1.409	1.105 1.797
LS score*	-0.036	0.140	0.797	-0.020	0.965	0.733 1.269
Model 4: PLS modes ($N_{latent}=10$) + Baseline model						
EDVI score*	0.839	0.161	<.0001	0.463	2.315	1.688 3.175
Sphericity score*	-0.172	0.113	0.126	-0.095	0.842	0.675 1.050
EF score*	0.092	0.129	0.474	0.051	1.096	0.852 1.411
RWT score	-1.809	0.178	<.0001	-0.998	0.164	0.115 0.232
Conicity score*	-0.390	0.122	0.001	-0.215	0.677	0.533 0.859
LS score	-0.668	0.142	<.0001	-0.368	0.513	0.389 0.677

488 All the modes are adjusted for age, gender, BMI, SBP, smoking status and diabetes history. *p<0.05

490

Table 9 Comparison of the four logistic regression models

	Deviance	AIC	BIC	AUC
Baseline Model	1559	1573	1614	0.7441
Index model	704	730	804	0.9596
PCA model	606	632	707	0.9728
PLS model ($N_{latent}=1$)	569	595	669	0.9738
PLS model ($N_{latent}=10$)	686	712	786	0.9599

491

AIC = Akaike information criterion ; BIC =Bayesian information criterion; AUC =Area under the ROC curve.

1
2
3
4
5
6
7
8
9
10
11
12
13
14
15
16
17
18
19
20
21
22
23
24
25
26
27
28
29
30
31
32
33
34
35
36
37
38
39
40
41
42
43
44
45
46
47
48
49
50
51
52
53
54
55
56
57
58
59
60
61
62
63
64
65

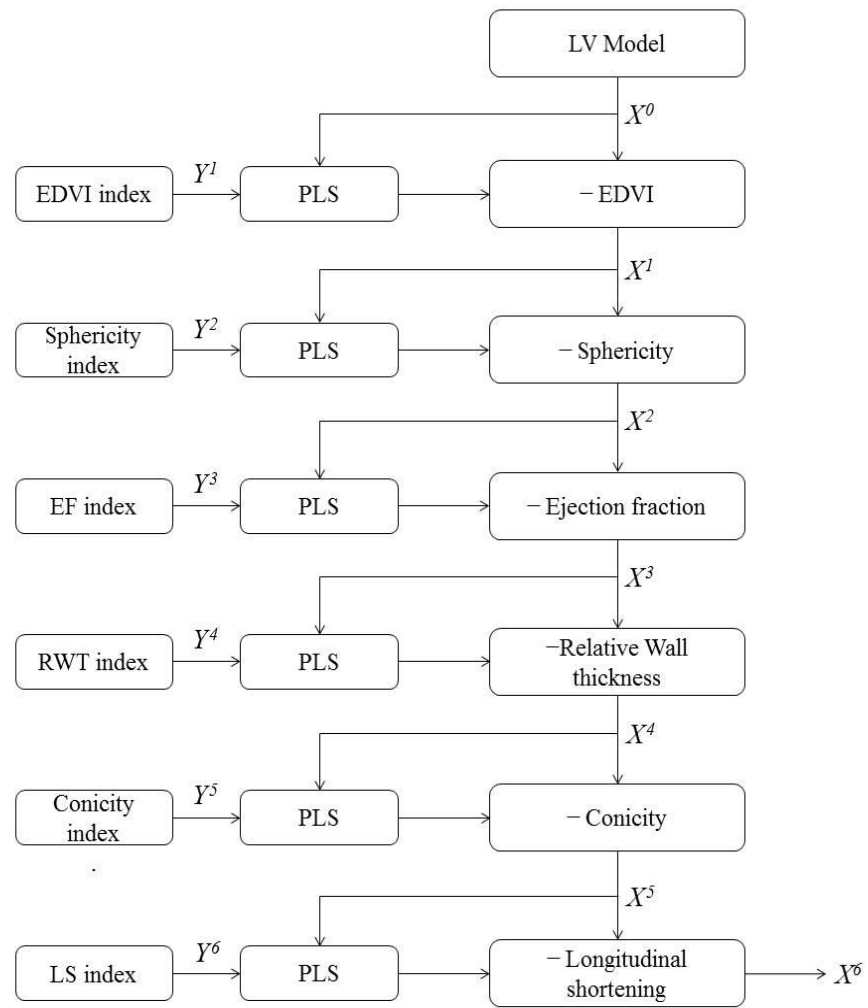


Figure 1 Data processing flow chart

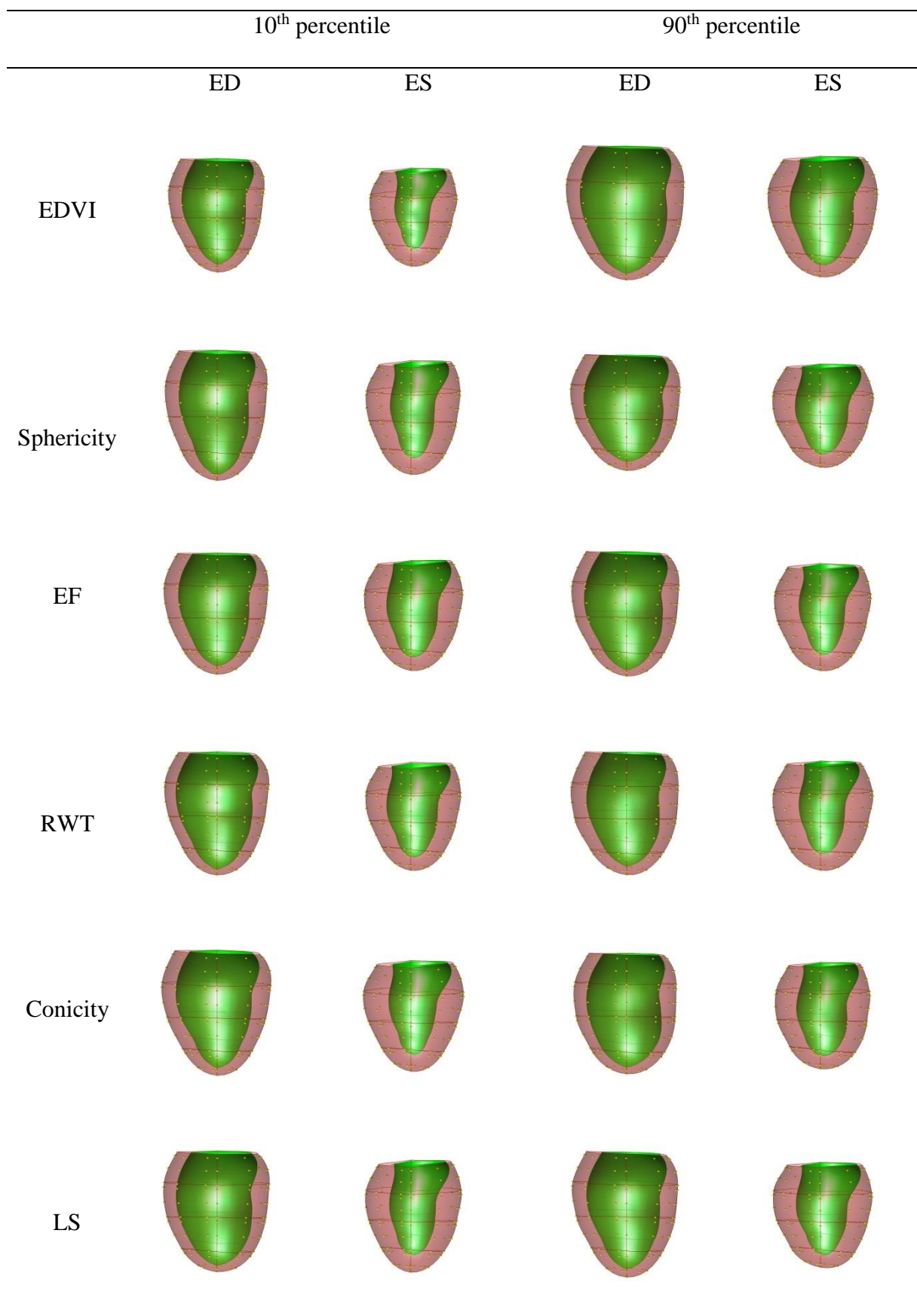


Figure 2 Plot of the PLS clinical components ($N_{latent}=1$)

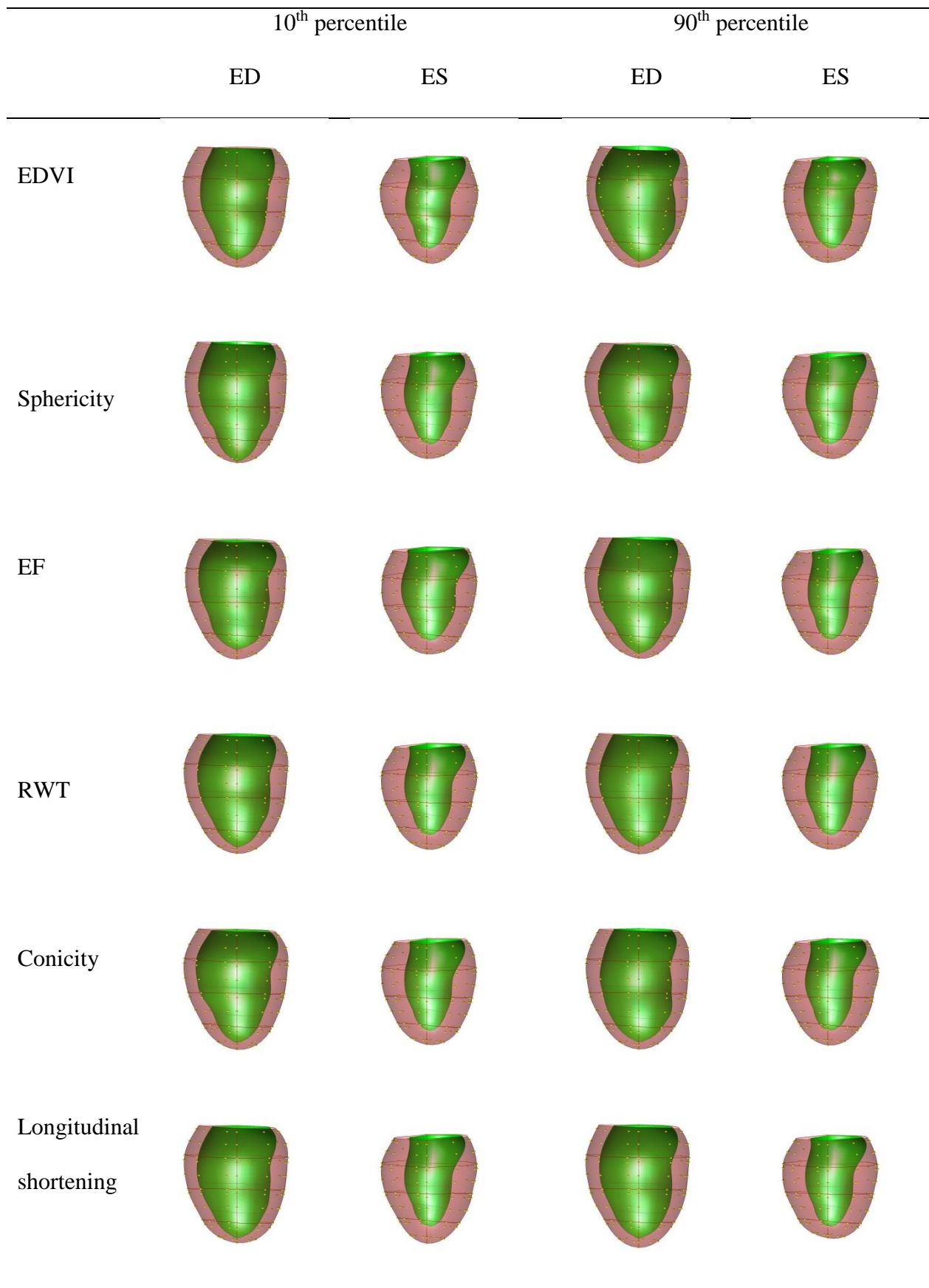


Figure 3 Plot of the PLS clinical components ($N_{latent}=10$)

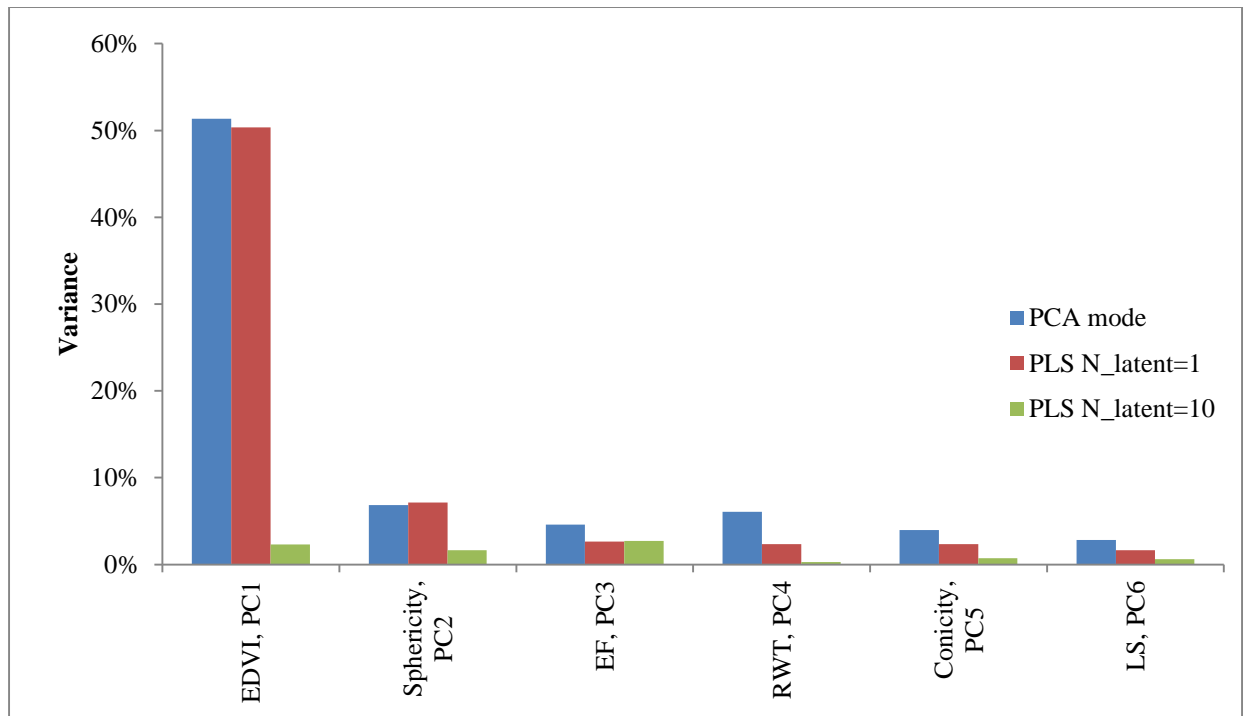


Figure 4 Variance explained by each PLS component and PCA component

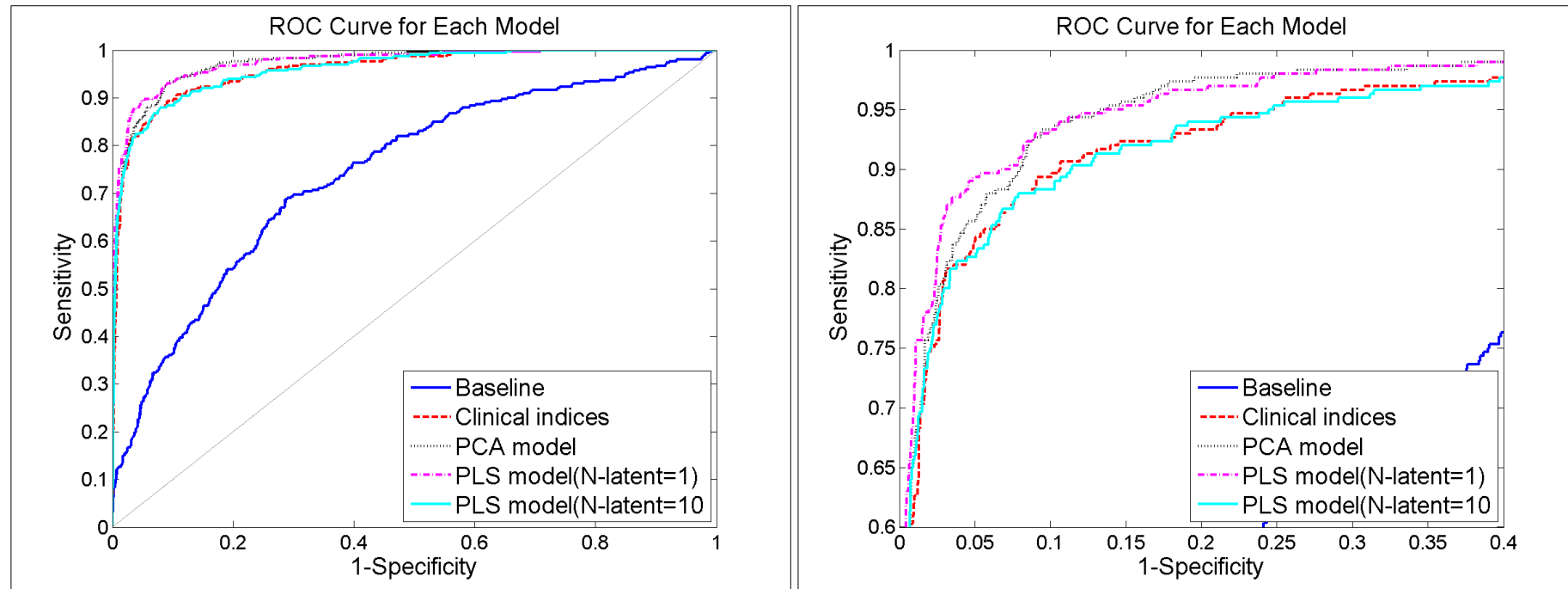


Figure 5 ROC curves for the five logistic regression models. The right figure shows a zoomed-in view to demonstrate the differences between the four models.

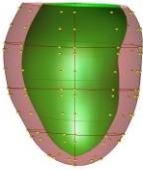
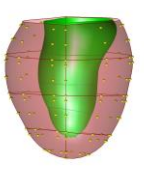
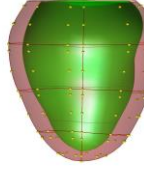
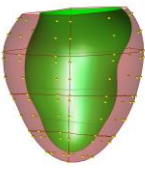
Asymptomatic		MI Patients	
			
ED	ES	ED	ES

Figure 6 Visualization of shape changes between volunteers and patients, using the combined PLS ($N_{latent} = 1$) component. Plots show the median LR score for the volunteer and patient groups respectively.